PAPER

Mean-field models for the chemical fueling of transient soft matter states†

Sven Pattloch (ID) [ab] and Joachim Dzubiella (ID) *[ab]

The chemical fueling of transient states (CFTS) is a powerful process to control the nonequilibrium structuring and the homeostatic function of adaptive soft matter systems. Here, we introduce a simple mean-field model of CFTS based on the activation of metastable equilibrium states in a tilted 'Landau' bistable energy landscape along a coarse-grained reaction coordinate (or 'order parameter') triggered by a nonmonotonic two-step chemical fueling reaction. Evaluation of the model in the quasi-static (QS) limit-valid for fast system relaxation-allows us to extract useful analytical laws for the critical activation concentration and duration of the transient states in dependence of physical parameters, such as rate constants, fuel concentrations, and the system's distance to its equilibrium transition point. We apply our model in the QS limit explicitly to recent experiments of CFTS of collapsing responsive microgels and find a very good performance with only a few global and physically interpretable fitting parameters, which can be employed for programmable material design. Moreover, our model framework also allows a thermodynamic analysis of the energy and performed work in the system. Finally, we go beyond the QS limit, where the system's response is slow and retarded *versus* the chemical reaction, using an overdamped Smoluchowski approach. The latter demonstrates how internal system time scales can be used to tune the time-dependent behavior and programmed delay of the transient states in full nonequilibrium.

I. Introduction

The transient assembly and ordering of active materials fueled by a chemical reaction is a key process in the nonequilibrium structuring and function of biomolecular systems, *e.g.*, to perform work or reach homeostatic mechanical responses.[1,2] These versatile and adaptive material features have triggered plenty of research recently, on one hand, to understand the fundamental physical properties of nonequilibrium transient states, but also, on the other hand, to develop synthetic active materials which display biomimetic or other novel useful behavior, driven by fuel consumption through chemical reaction networks.[3–10] Experimental examples are the fuel-driven self-assembly of synthetic molecules into fibers[11] or gels[12,13] with variable and controllable lifetime and stiffness, the fueled nucleation and coacervation[14] and spinodal decomposition[15]

in phase separating systems, as well as the fueled collapse of functional macromolecules such as hydrogel colloids.[16,17]

The desired goal of the ongoing research efforts is to establish rational design principles that enable a generic access to nonequilibrium soft matter systems with adaptive and predicable dynamics,[6,18] for example, to demonstrate programmable hydrogel-based model systems.[19,20] Hydrogels are soft, responsive and deformable, and thus of special interest for the development, *e.g.*, of chemically fueled mechanical actuators.[21,22] However, realizing programmable or even adaptive structural dynamics has proven challenging because it requires harmonization of the chemical energy uptake and dissipation events within the steady states.[9] The full nonequilibrium is even more difficult to control due to the intricate coupling of the time-dependent chemical, thermodynamic, as well as mechanical degrees of freedom of the supramolecular systems.[3,4,23] The theoretical modeling is therefore often either too complex to derive simple laws, or relies only on the numerical solution and phenomenological interpretation of the underlying chemical networks.[10,15,17,24] The latter typically disregard the coupling to the emerging mechanical or structural (order) parameters during the spatiotemporal evolution of the whole system to converge to a holistic modeling approach.

Here, we make a first step towards a simple theoretical treatment of the coupling of the chemical fueling to the

[a] *Applied Theoretical Physics-Computational Physics, Physikalisches Institut, Albert-Ludwigs-Universität Freiburg, D-79104 Freiburg, Germany. E-mail: joachim.dzubiella@physik.uni-freiburg.de*

[b] *Cluster of Excellence livMatS@FIT-Freiburg Center for Interactive Materials and Bioinspired Technologies, Albert-Ludwigs-Universität Freiburg, D-79110 Freiburg, Germany*

emerging structure, thermodynamics and mechanics of the system within a generic model framework. The latter is motivated by a Landau-type of mean-field model which was historically introduced to access the qualitative behavior of phase transitions, *e.g.*, as of magnetic systems in external fields.[25] Since often we consider state- or phase-switching systems, it makes sense to use the Landau model as a starting point. In particular, we assume that the fueled system is to some degree bistable (two-state), featuring a stable state and a highly unstable state, the latter of which can then be activated by an external field. We further assume that the chemical fueling acts like an energetic field which can modify the Landau energy landscape. In other words, fueling increases the probability of the unlikely 'hidden' state over the initial state for a certain time, thus stabilizing a transient state with variable lifetime. In contrast to the classical Landau model, the external field enters in our approach through the action of a time-dependent chemical reaction (or chemical network). As a first approximation, the field enters linearly into our model analogous to the popular *m*-value approach to describe biomolecular state transitions; here, the Gibbs free energy of a two-state protein unfolding/denaturation is modified by interface free energy changes through ad- or desorption of cosolutes[26–28] or the change of electrostatic intra-polymer interaction energies.[29]

We apply and exemplify the usefulness of our model in the quasi-static (QS) limit (where system relaxation is fast compared to the chemical reaction) explicitly to fit the experimental data of chemical fueling of hydrogel collapse recently put forward by Heckel *et al.*[16] In these experiments, the chemical fuel *N*-ethyl-*N*′-(3-dimethy-laminopropyl)carbodiimide (EDC) was used to trigger the volume phase transition (VPT) for poly(methacrylic acid) (PMAA) microgels, to demonstrate that the collapsed hydrophobic state can be programmed in time using the fuel concentration in a cyclic reaction network. The EDC addition enables two neighboring carboxylic acid groups to form a cyclic carboxylic anhydride which increases the hydrophobicity of the hydrogel, leading to a time-dependent collapse and swelling dynamics. The measured time-dependent observable was then the mean finite hydrogel radius $R(t)$, averaged over an ensemble of particles in dilute solution for fixed time t.

Although simple and mean-field, we demonstrate at hand of this explicit case study of transiently collapsing hydrogels that many useful scaling laws can be drawn from our model already in the QS limit, in particular, for the relations between fuel concentration, chemical rates, and the duration of the transient states between the equilibra. Moreover, we show that, like in the Landau framework,[25] such a Hamiltonian-based model can then also be employed by using simple diffusive relaxational dynamics to study a full nonequilibrium fueling process. This is relevant in situations when the chemical and the system time scales are comparable and temporal effects like delay and retarded response come into play. We discuss further possible applications and extensions of these models in the final outlook section of this work.

II. General model

A. Coarse-grained bistable Hamiltonian

In our model, the fueled system is described by a coarse-grained one-dimensional reaction coordinate, Q, *e.g.*, the instantaneous radius of a single responsive particle, *cf.* Fig. 1, or, in general, any meaningful structural (order) parameter. In order to allow for state transitions of the system (as, *e.g.*, in the hydrogel volume transition,[30,31]) the coordinate is assumed to live in a bimodal energy landscape, $\mathcal{H}_0(Q) = A(\Delta Q)^2 + B(\Delta Q)^4$, which we model by a simple quartic form as put forward in the simplest case by Landau to model phase transitions.[25] Here, $\Delta Q = Q - Q_c$, and A, B, and Q_c describe the intrinsic energy landscape, with Q_c being the center of the symmetric quartic form. For $A < 0$ and $B > 0$ it exhibits two local minima at Q_1 and Q_2. If Q is, for example, a particle volume or size, then the interpretation of such a Hamiltonian would be that it essentially represents a nonlinear elastic energy including a volume transition.

The action of the chemical fuel is considered by a time-dependent energy contribution $\mathcal{H}_p(Q, t) = m \times (p(t) - p^*)\Delta Q$, which both Q and the product concentration $p(t)$ enter linearly, like an external magnetic field in the Landau picture. The products are generated by the fuel by a chemical reaction and modify the energetics of the system. The total form of the Hamiltonian is thus

$$\begin{aligned}\mathcal{H}(Q,t) &= \mathcal{H}_0(\Delta Q) + H_p(\Delta Q, t)\\ &= A(\Delta Q)^2 + B(\Delta Q)^4 + m \cdot (p(t) - p^*)\Delta Q.\end{aligned} \quad (1)$$

The value of m defines the strength of the action of the chemical products p. For the critical concentration p^* the chemical contribution $\mathcal{H}_p(Q)$ vanishes and the two coarse-grained states are equally probable. In other words, p^* describes the initial bias (tilt) of the bimodal landscape in equilibrium. The Hamiltonian (1) is explicitly time-dependent because of the time-dependent product concentration $p(t)$. The increase of the latter leads to large tilts of the landscape, activating metastable states into transient probable states, *cf.* Fig. 1.
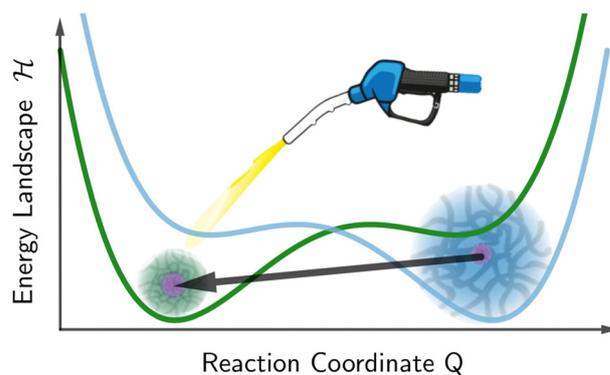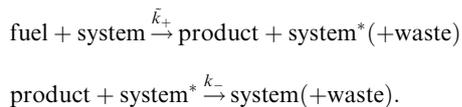

Fig. 1 Landau like energy landscape $\mathcal{H}(Q)$ along a reaction coordinate Q, exemplified for the radius R of a spherical hydrogel particle with small (greenish hydrogel) and big (blueish hydrogel) states. The fueling leads to a tilt of the equilibrium landscape (blue line) and transiently stabilizes the small state in the activated landscape (green line).

A few notes on the model assumptions are in order: a linear change of thermodynamic two-state energies is not always justified but it is simple and can almost always be derived from a Taylor expansion as a first order correction of external energetic field contributions. Importantly, in the field of polymeric state transitions, a linear potential is established and well accepted within the 'm-value' framework for the action of simple cosolutes on the coil-to-globule (or folding/unfolding) transition in bio- and polymer physics.[26–28] The chemical 'field' of physically binding cosolutes leads to interfacial free energy changes, expressed in magnitude through m, and can thus be included as part of the total (Gibbs) free energy. In charged systems, salt and electroneutralizing chemically binding molecules (such as protons) lead to changes in the electrostatic contribution to the total free energy, which can also be included and taylored to linear potentials.[29] In that sense $mp^\star$ in the equation above can also be interpreted as a thermodynamic distance to the (coil-to-globule or volume) transition temperature T_{crit} and is essentially related to a temperature difference $\propto T - T_{crit}$ times transition entropy.[28] In other words, for a certain responsive system with a thermodynamic transition temperature, the initial tilt $p^\star$ can be pre-designed by temperature, transition entropy, and the chemistry specific m-value, which are often known or measurable quantities.

B. Chemical fueling reaction

The chemical fueling is assumed to follow effectively a simple two-step reaction process

$$\text{fuel} + \text{system} \xrightarrow{\tilde{k}_+} \text{product} + \text{system}^*(+\text{waste})$$

$$\text{product} + \text{system}^* \xrightarrow{k_-} \text{system}(+\text{waste}).$$

Here, the fuel, $f(t)$, is converted in the homogeneous solution to a product, $p(t)$, binding at and modifying the considered system, $e.g.$, the hydrogels, with a rate constant $\tilde{k}_+$. The products in the modified system* decay with a rate constant k_-. Such a simple two-step reaction follows the rate equations

$$\begin{aligned} \dot{f}(t) &= -\tilde{k}_+ f(t)[p_{sat} - p(t)] \\ \dot{p}(t) &= \tilde{k}_+ f(t)[p_{sat} - p(t)] - k_- p(t), \end{aligned} \qquad (2)$$

with the starting conditions $f(t=0) = f_0$ ($i.e.$, the initial fuel concentration) and no product initially, $p(t=0) = p_0 = 0$. The product is the species that is active, in the sense that it changes the system by physically/chemically binding to it. Typically, the product has only a certain lifetime and decays with a first order rate k_-. Note that the $\tilde{k}_+$ is a second order rate, (because the system has a concentration of binding sites,) which we denote by the tilde symbol. Moreover, we impose a saturation concentration, p_{sat}, to account for the effect of a finite maximal number of products because of limited binding sites. In equilibrium, $\dot{p} = 0$, we recover the Langmuir isotherm for the function $p(f)$ with equilibrium constant $\tilde{k}_+/k_-$.[32] During time evolution, the products reach a single maximum, $p_{max} := \max(p) \leq p_{sat}$, as further exemplified below.

Generally, we can distinguish various regimes depending on whether the ratio of fuel to p_{sat} and the ratio of $\tilde{k}_+ p_{sat}$ to k_- is low/high. In a related discussion by Sharko $et\ al.$[10] it is shown that to activate the transient state, we need either very high fuel concentrations, or higher activation than deactivation rates in order to obtain sufficiently many active products. We will quantify this more in the following for our model. Since we focus on systems with controllable lifetime we restrict ourselves to the activation dominant case $\tilde{k}_+ p_{sat} > k_-$.

Analytic solutions for $p(t)$ we only obtain for the unsaturated case $p_{sat} \gg p$ for all times, where we can approximate $p_{sat} - p \simeq p_{sat}$ and introduce a new pseudo first order rate constant $k_+ = \tilde{k}_+ p_{sat}$. The analytical solution is then analogous to the double-exponential two chain reaction of radioactive decay[33]

$$p(t) = \frac{k_+ f_0}{k_+ - k_-}\left(e^{-k_- t} - e^{-k_+ t}\right). \qquad (3)$$

In this case, the time evolution of products $p(t)$ shows an exponential rise with rate k_+ at the beginning, a maximum at p_{max} at $t = t_{max}$, following a decay with rate k_- for long times. This is exemplified in Fig. 2, where we compare different fueling situations. The time where the product concentration is maximal in the unsaturated (us) case is given by

$$t_{max}^{(us)} = \frac{\ln \kappa}{k_- - k_+} \qquad (4)$$

with the corresponding maximum product concentration

$$p_{max}^{(us)} = p(t_{max}^{(us)}) = \frac{f_0}{1 - \kappa}\left(\kappa^{\frac{\kappa}{1-\kappa}} - \kappa^{\frac{1}{1-\kappa}}\right), \qquad (5)$$

where we introduced $\kappa = k_-/k_+$, the ratio of the rates with $0 < \kappa < 1$. The analytical solutions for the unsaturated case are compared to numerical solution of eqn (2) for saturated situations in Fig. 2. The saturated cases in these examples show suppressed peaks and plateau-like behaviors where $p \leq p_{max} < p_{sat}$ and always $p_{max} < p_{max}^{(us)}$.
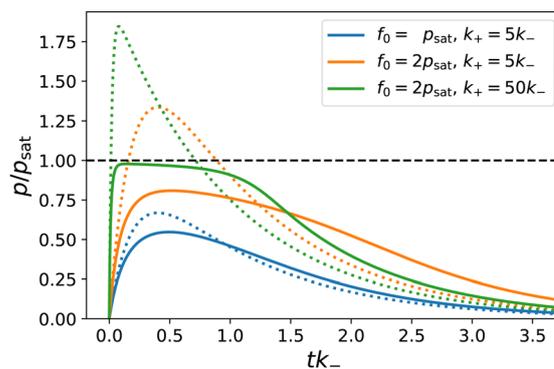

Fig. 2 Product concentration $p(t)$ (scaled by p_{sat}) for different parameter settings. Solid lines are according to the numerical solutions of eqn (2). Dotted lines show the concentration profiles for the same parameters without saturation, following the analytical solution, eqn (3). Besides the initial fuel concentration f_0 we vary k_+, $cf.$ legend.

C. Quasi-static (QS) chemical fueling

1. Equilibrium averages. If the reaction coordinate Q relaxes much faster than the chemical timescales, the dynamics are quasi-static (QS), *i.e.*, the Boltzmann distribution of Q

$$\rho(Q, t) = \exp(-\beta\mathcal{H}(Q, t))/Z(t) \qquad (6)$$

according to the Hamiltonian (1) holds for every time t. The normalizing (canonical) partition sum is

$$Z(t) = \int e^{-\beta\mathcal{H}(Q,t)}dQ. \qquad (7)$$

The average value of a function $X(Q, t)$ then directly follows from the Boltzmann average

$$\langle X(t)\rangle = \int X(Q, t)\rho(Q, t)dQ. \qquad (8)$$

Hence, in the QS limit we can straightforwardly consider also thermodynamic quantities such as energy $U(t) = \langle\mathcal{H}\rangle$, the (Helmholtz) free energy $F(t) = -k_BT\ln Z(t)$, entropy $S(t) = (U(t) - F(t))/T$, and the power $P = dF/dt$. Using the exact relation $dF/dt = \langle d\mathcal{H}/dt\rangle$, one can derive the useful relation for our model that the power is

$$P = m(dp/dt)\langle\Delta Q(t)\rangle, \qquad (9)$$

i.e., given by the change of the time evolution of the product times the time-dependent mean of the order parameter. The initial fueling power is then provided by $P(t = 0) \simeq mf_0k_+(Q_2 - Q_c)$ if we use $\langle\Delta Q(t = 0)\rangle \simeq Q_2 - Q_c$.

We note that the free energy F above is considered as the contribution stemming from the Q-state distributions, in excess over the constant ideal gas translation contributions, or other constant contributions not depending on Q. Experimentally, the constant-pressure Gibbs ensemble would be more appropriate rather than the Helmholtz ensemble we use here. However, we neglect the volume work term because we assume that its contribution at normal conditions (1 bar) are negligible compared to the relevant changes in the intrinsic energy landscape $\mathcal{H}$.

2. Separation of the energy contributions. The time-dependent work and energy can be deeper analyzed by considering the contributions to the Hamiltonian, eqn (1). It consists of two parts. First, we have the intrinsic part

$$\mathcal{H}_0(Q) = A(\Delta Q)^2 + B(\Delta Q)^4 - mp^*\Delta Q, \qquad (10)$$

which does not depend on the external field, and then a second part creating the time-dependent linear chemical contribution

$$\mathcal{H}_{chem}(Q, t) = mp(t)\Delta Q. \qquad (11)$$

By calculating the average values

$$U_0(t) = \int\mathcal{H}_0(Q)\rho(Q, t)dQ \qquad (12)$$

and

$$U_{chem}(t) = \int\mathcal{H}_{chem}(Q, t)\rho(Q, t)dQ, \qquad (13)$$

respectively, we can thus divide the energy in its intrinsic and external contributions. For many experimentally relevant systems we can interpret them as mechanical (U_0) and chemical (U_{chem}) contributions, respectively. For Q being, for example, the particle size, the first one describes the elastic energy which changes over time only by variations of the particle distributions, while the second one depends directly on the time caused by the variable chemical product concentration $p(t)$.

3. Duration of transient states. We now estimate the duration of transient states for our 2-state model in the QS limit. We can call the transient state 'activated' if its probability of occurrence is larger than the other, initial state. We recognize that in the QS limit a minimum threshold of fueling concentration is needed to activate the transient state, given by the conditions $p(t) = p^*$ with $p_{max} \geq p^*$. A full analytical solution for eqn (2) is apparently not possible, but we can use the unsaturated case in the limit $p_{sat} \gg p^*$. Then, we obtain by setting eqn (5) to p^* the approximative threshold (or 'critical') concentration for successful fueling

$$
\begin{aligned}
f_{0,crit} &= \frac{p^*(k_+ - k_-)}{k_+}\left[\left(\frac{k_+}{k_-}\right)^{\frac{k_-}{k_- - k_+}} - \left(\frac{k_+}{k_-}\right)^{\frac{k_+}{k_- - k_+}}\right]^{-1} \\
&= p^*(1 - \kappa)\left(\kappa^{\frac{\kappa}{1-\kappa}} - \kappa^{\frac{1}{1-\kappa}}\right)^{-1}
\end{aligned} \qquad (14)
$$

which in the typical limit of $k_- \ll k_+$ reduces to the simple relation $f_{0,crit} = p^*$. As discussed above, p^* signifies the important initial thermodynamic distance of the system to the transition point and can in principle be *a priori* designed. Once fixed, it directly defines the threshold concentration for successful fueling. Obviously, also $p_{sat} > p^*$ should hold for successful activation.

If we are above the threshold concentration for fueling, we can analytically estimate the duration of the times of the transient states. This we can do in two ways:

(i) Symmetry definition of the transient time

In the case of a sufficiently high saturation limit, $p_{sat} > p^*$, and the condition $p(t) > p^*$ holds, the stability bounds of the transiently stable state are very well defined by the times t_1 and $t_2 > t_1$ where $p(t) = p^*$, *i.e.*, where the Hamiltonian is symmetric in Q around Q_c and the two states are equally likely. (Note again that in our simple two-step chemical reaction the condition $p(t) = p^*$ is met only twice, during on-fueling and decay.) The duration of the transient state can then be formally defined as

$$\tau_{trans} = [t_2 - t_1]_{p=p^*} \qquad (15)$$

where the notation means that the two times are evaluated if $p(t) = p^*$. We find through the slow-decay approximation $e^{-k_- t_1} \approx 1$, that

$$t_1 = -\frac{1}{k_+}\ln\left(1 - \frac{p^*(k_+ - k_-)}{k_+f_0}\right), \qquad (16)$$

and the fast-fueling assumption $e^{-k_+ t_2} \approx 0$, that

$$t_2 = \frac{1}{k_-}\ln\left(\frac{k_+f_0}{p^*(k_+ - k_-)}\right), \qquad (17)$$

the duration of the transient state is essentially (and not surprisingly)

determined by the on and off-rates of fueling, $\tau_{\text{trans}} \sim (1/k_- - 1/k_+)$, while there are logarithmic corrections depending on all rates and densities f_0 and p^*.

Interestingly, we can show that for a bistable Hamiltonian of form (1) the times defining the transient states at $p(t) = p^*$ are extrema of thermodynamic state functions, such as the free energy. Taking the derivative of the partition function Z with respect to p, we find

$$\frac{dZ}{dp} = -\int_{-\infty}^{\infty} mQ e^{-\left(AQ^2 + BQ^4 + m(p(t)-p^*)Q\right)} dQ. \tag{18}$$

Obviously, the integrand becomes an antisymmetric function if $p(t) = p^*$ so that the integral vanishes and Z has an extreme point, more precisely, leading to a maximum of the free energy $F(t) = -k_B T \ln Z(t)$. Using the modified Bessel functions of the second kind $K_z(x)$, we can write the extremum of the free energy:

$$F_{\text{max}} = F(p^*) = -k_B T \left[\frac{A^2}{8B} + \ln\left(\frac{K_{\frac{1}{4}}\left(\frac{A^2}{8B}\right)}{2\sqrt{-\frac{B}{A}}} \right) \right] \tag{19}$$

(a detailed derivation can be found in the ESI†) which in the QS limit constitutes the maximum work the system can perform.

(ii) Plateau definition of the transient time

In the case of strong saturation (that is, small $p_{\text{sat}} < p_{\text{max}}^{(\text{us})}$), we obtain a longer period of a plateau behavior, for which $p(t) \simeq p_{\text{sat}} = p_{\text{max}}$. Then the duration period of the transient state is mostly given by the time spent in the plateau. This we can estimate by the following: at the plateau we have $p \simeq p_{\text{sat}} = $ constant and thus $\dot{p} = \dot{f} - k_- p \simeq 0$, *cf.* eqn (2), and a linear decrease of the remaining fuel $f(t) \simeq f_0 - k_- p_{\text{sat}} t$. The plateau decays when most of the fuel is consumed $f(t) \ll f_0$. Hence, we find for the duration of the plateau approximately

$$\tau_{\text{trans}} \propto \tau_{\text{plateau}} \simeq \frac{f_0}{k_- p_{\text{sat}}}, \tag{20}$$

constituting a useful law in dependence of the initial fuel concentration, decay rate, and saturation concentration. Noteworthy the transient time is now simply linear in f_0, if a plateau (*i.e.*, saturation) behavior dominates the system. Due to the approximations made, however, a constant offset in this formula is generally plausible.

Note also that for saturating systems, the symmetry definition (i) should lead to values very close to the plateau definition (ii). The symmetry definition is more general and holds also for non-saturating systems, while for both $p > p^*$. Only the plateau behavior (ii) leads to the clear linear scaling given by eqn (20).

D. Slow system relaxation: Smoluchowski approach

If the system relaxation is slow compared to the chemical reaction, its response to the time-dependent Hamiltonian will be retarded. As a simple start, we can assume the system is following an overdamped diffusive dynamics following the Smoluchowski (drift-diffusion) equation:[34,35]

$$\frac{\partial \varrho}{\partial t} = D\frac{\partial^2 \varrho}{\partial Q^2} - D\beta\left[\frac{\partial^2 \mathcal{H}}{\partial Q^2}\varrho + \frac{\partial \mathcal{H}}{\partial Q}\frac{\partial \varrho}{\partial Q}\right] \tag{21}$$

where $\varrho = \varrho(Q,t)$ is the time-dependent probability distribution, D the diffusivity which we assume Q-independent and sets the intrinsic hydrogel relaxation time scale. We solve this equation numerically using the *fplanck* python package.[36] Note that time-dependent averages in the system can be still evaluated with general eqn (8).

For an interpretation of the results during slow dynamics we need to briefly discuss the timescales in this problem: A diffusion timescale can now be defined by $\tau_D = (Q_2 - Q_c)/D$, where Q_2 is the position of the initial global minimum of $\mathcal{H}(Q)$. Note, that this position changes slightly over time as the linear term of the Hamiltonian does. For our definition, we thus use the symmetric situation at $p(t) = p^*$ where it holds that $\tau_D = -\frac{A}{2BD}$. This time expresses how long the system needs to diffuse from the minimum to the barrier position.

A reasonable quantity putting in relation the reactions and the diffusive time scale is the dimensionless second Damköhler number[37] which we define as

$$\alpha = \tau_D k_+. \tag{22}$$

If $\alpha \ll 1$, we are in the QS limit. For $\alpha \gtrsim 1$ the system relaxes slow and significantly retarded to the chemical reaction. In the extreme case of $\alpha \gg 1$, the system never relaxes during fueling and essentially does not change in time.

Another relevant timescale in this bistable system, if energy barriers are significant $\left(\Delta \mathcal{H} \gtrsim k_B T\right)$, is the so-called Kramers time for diffusive barrier crossing.[38,39] There are several expressions for it depending on the approximations made. For simplicity, we define the Kramers time with τ_D as a prefactor to the important exponential Arrhenius-factor to have it consistent in the vanishing barrier limit, hence,

$$\tau_{\text{Kramers}} = \tau_D e^{\beta \Delta \mathcal{H}}, \tag{23}$$

with energy barrier $\Delta \mathcal{H}$. (For the interested reader, in eqn (S10) of the ESI† we define the Kramers time with the more conventional prefactor considering the curvatures of the energy landscape, and plot a comparison in Fig. S8, ESI†) For large barriers, the Kramers time is limiting for the distribution to flood the metastable state once activated by the fuel, and also for the reverse process. Note that $\Delta \mathcal{H}(t)$ as well as the location of the extrema are themselves time-dependent meaning that also the crossing time is in general time-dependent and not very well defined. For simplicity, we follow the rule that we calculate the Kramers time using $\Delta \mathcal{H} = \mathcal{H}(Q_c) - \mathcal{H}(Q_2)$ from the symmetric, non-skewed energy landscape at $p = p^*$. The ratio between Kramers time and the chemical fueling time, we denote then by $\alpha_K = \tau_{\text{Kramers}} k_+$.

III. Case study: chemical fueling of hydrogel collapse

We now apply our model in the QS limit to explicitly fit the experimental data of chemical fueling of hydrogel collapse recently put forward by Heckel et al.,[16] as described in the Introduction. The measured observable was the finite hydrogel radius $R(t)$, see Fig. 3, averaged over many particles for fixed time t. We consider $R(t) = \langle Q(t) \rangle$ as an ensemble average over a hypothetically infinitely large sample of spheres.

A. Fitting procedure

Our fit is based on the numerical solution of the coupled eqn (1) and (2) including saturation. The EDC fuel concentration is translated to f_0 in units of 1 mmol l^{-1}. In Heckel et al. we find several measurement curves for two pH-values, pH = 6.1 and pH = 7.2, with differing initial fuel concentration f_0. We reconcile our model and the experimental data by minimizing the total mean squared deviations (MSD) between theory curves and experimental data for a fixed pH (details in the ESI†). The model takes the initial fuel concentration f_0 as an input, while the other parameters listed in Table 1 are fitting parameters, now with real experimental units assigned. However, all of the fitting parameters are kept constant for a fixed pH value.

When a fitting parameter is called *global*, it means that it is constant also for both pH values.

We treat the parameters for the energy landscape A, B and Q_c as global parameters, because we expect them to be intrinsic properties of the hydrogel colloids, which do not depend on the pH-value. We also globally fix p_{sat}, which should be constant because pH-dependent side reactions changing the amount of binding sites in the microgels are not included in our model. In contrast, the chemical reaction rates[40,41] and also the m-value describing their impact on the energy landscape may depend on the pH-value. (We note that removing the constraints of pH-independent energy landscape parameters we obtain slightly improved fits, but because the improvement is only little (see ESI† Fig. S1), we consider a pH-dependent m-value as sufficient.)

Moreover, we observe some arbitrariness (*i.e.*, some insensitivity) of the fits regarding the precise magnitude of the energy barrier. We avoid this problem by fixing the energy barrier for a fixed pH through the exact expression in the symmetric landscape, $\Delta\mathcal{H} = \dfrac{A^2}{4B}$. Interestingly, unimodal potentials of the simple form $\propto \Delta Q^{2n}$ with $n = 1,2$ were not able to reproduce the relatively fast sigmoidal transitions from one state to the other (see ESI† Fig. S2 and S3). Improved fits were achieved by broader $n = 3$ and a square-well 'box' potential. But here the radius distribution functions become relatively broad, in contrast to the
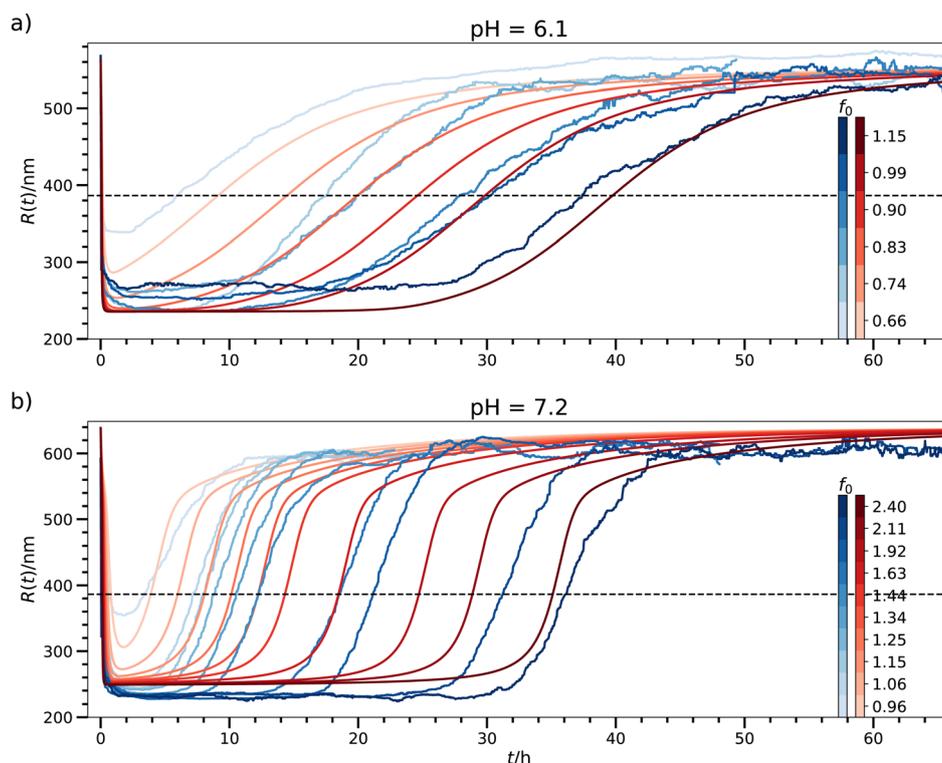

Fig. 3 Model fits for a fixed energy barrier of $2k_BT$ to the data set of chemically fueled hydrogel collapse[16] in the QS limit for (a) pH = 6.1 and (b) pH = 7.1. The color bar codes the different fueling concentrations f_0. The blueish hues represent the experimental and the reddish ones the theoretical data. The horizontal dashed line indicates the radius at the symmetric state, $R(p^*)$, below which the transient state is activated. Note that in contrast to the original work by Heckel et al.[16] we choose f_0 in units of mmol l^{-1}, but not in 'equivalent EDC' which is stoichiometrically scaled by twice the concentration of carboxylic acid groups. These units can be converted *via* 1 equiv. EDC = 0.96 mmol l^{-1}.

Table 1 Model parameters with corresponding units for the fits of the experimental data of Heckel et al.[16] presented in Fig. 3. f_0 is input from experiments, while the others are global or pH-dependent fitting parameters, see text and Table 2

	Unit	Description
A	$k_{\mathrm{B}}T\,\mathrm{nm}^{-2}$	Bimodal energy landscape parameter
B	$k_{\mathrm{B}}T\,\mathrm{nm}^{-4}$	Bimodal energy landscape parameter
Q_{c}	nm	Center of symmetric energy landscape
m	$k_{\mathrm{B}}T\,\mathrm{lmmol}^{-1}\,\mathrm{nm}^{-1}$	Impact of p on the energy landscape
$\tilde{k}_+$	$\mathrm{l\,mmol}^{-1}\,\mathrm{h}^{-1}$	p-Forming rate
k_-	h^{-1}	p-Decomposition rate
p_{sat}	$\mathrm{mmol\,l}^{-1}$	Saturation value for p
$p^\star$	$\mathrm{mmol\,l}^{-1}$	Initial skew/transient threshold
f_0	$\mathrm{mmol\,l}^{-1}$	Initial fuel concentration (taken from experiment)

experiments,[16] with unrealistically unbound values of the radius R. Hence, a Landau-like quartic potential including the presence of transition barriers $(\Delta\mathcal{H} \gtrsim k_{\mathrm{B}}T)$ was most adequate to fit the data. Note that hydrogel charge content can tune the location and the width of the VPT.[30]

Further modifications of the fitting constraints are conceivable. For example, we can pre-fix p_{sat} to the number of available reaction partners, allow an offset for f_0, or change pH-dependent variables to global ones. Similarly, we tested purely unsaturated equations for p, eqn (3), but dropped them due to the following reasons. Without saturation, the maximum value of p is not bounded but can exceed the (experimentally roughly known) number of reaction partners. In addition, the pronounced peaks in $p(t)$ without saturation make it hard to reproduce the flat plateaus we observe in $R(t)$ for large f_0 (see Fig. 2). Finally, without saturation the fast conversion to p and thus enhanced fuel consumption leads to a sublinear scaling between f_0 and the transient time, which is in contrast to the fully linear experimental observation, cf. Fig. 5 later.

B. Fitting results

The results of an exemplary best fit are displayed in Fig. 3. Here, we fixed the energy barrier to $2\,k_{\mathrm{B}}T$. We obtain comparable results using other energy barriers (see Fig. S6, ESI† for $\Delta\mathcal{H} = 5\,k_{\mathrm{B}}T$; fits based on potentials other than defined in eqn (1) can also be found in the ESI†), which confirms that the exact choice of the barrier height is of minor importance in the QS case, as long as is it not vanishing $(\Delta\mathcal{H} \gtrsim 1\,k_{\mathrm{B}}T)$. Later we will see, however, that the precise value of $\Delta\mathcal{H}$ makes a substantial difference in the full nonequilibrium when the system relaxation is comparable to the chemical reaction times.

The parameters of this fit are summarized in Table 2. The fits themselves are not quantitative, but considering the relatively large error in the time domain of the experiments of a few hours (cf. Fig. 2b in Heckel et al.[16]), they are satisfactory, in particular, they agree very well in several qualitative aspects: They describe the fast drop of $R(t)$ in the experiments down to 236 nm and 224 nm for pH = 6.1 and 7.2, respectively (compared to the values obtained by our fits: 236 nm and 249 nm), the plateau behavior, the slow rise of the radius, and, in particular, the trends and magnitudes of the transient times, as in detail discussed later.

Note that our model fits allow to reversely calculate the time evolution of fuel $f(t)$ and/or products $p(t)$ in the system. For the

Table 2 Values of the resulting parameters for an optimal fit of the data for transient hydrogel fueling plotted in Fig. 3. A, B, Q_{c}, and p_{sat} are global, pH-independent fitting parameters. The last line separates k_+, Q_1 and Q_2 which are characteristic for our energy landscape but directly depend on some of the fitting parameters

	pH = 6.1	pH = 7.2
A $(k_{\mathrm{B}}T\,\mathrm{nm}^{-2})$	-1.89×10^{-4}	
B $(k_{\mathrm{B}}T\,\mathrm{nm}^{-4})$	4.45×10^{-9}	
Q_{c} (nm)	386	
m $(k_{\mathrm{B}}T\,\mathrm{l\,mmol}^{-1}\,\mathrm{nm}^{-1})$	6.87×10^{-2}	0.260
$\tilde{k}_+$ $(\mathrm{l\,mmol}^{-1}\,\mathrm{h}^{-1})$	25.5	11.9
k_- (h^{-1})	2.06×10^{-2}	5.79×10^{-2}
p_{sat} $(\mathrm{mmol\,l}^{-1})$	0.799	
$p^\star$ $(\mathrm{mmol\,l}^{-1})$	0.550	0.749
$k_+ = \tilde{k}_+ p_{\mathrm{sat}}$ (h^{-1})	20.4	9.53
$Q_1 = Q_{\mathrm{c}} - \sqrt{-A/2B}$ (nm)	241	
$Q_2 = Q_{\mathrm{c}} + \sqrt{-A/2B}$ (nm)	532	

parameter set of Fig. 3 and the exemplary choices pH = 6.1 and $f_0 = 0.99\ \mathrm{mmol\,l}^{-1}$, we show the temporal evolution of the products $p(t)$ together with the corresponding time evolution of the energy landscape $\mathcal{H}(Q, t)$ in Fig. 4. One can nicely compare the features of products and mechanical response at different characteristic times, including the saturation behavior and the symmetric states at $p = p^\star$.

More conclusions can be drawn from the fitting numbers in Table 2. Since $f_0/p_{\mathrm{sat}} \leq 2.5$, we expect high k_+/k_- ratios because of the pronounced plateaus. Indeed, our k_+ are about three orders of magnitude larger than k_-. This means, with respect to Sharko et al.,[10] we are moving through different fueling regimes depending on the initial fuel concentration f_0. In particular, our model captures the transition from small dips (minima) to ever-widening plateaus. Furthermore, we find that the expected pH-dependent reactivity changes with our parameters: when pH increases, we expect slower anhydride formation[40,41] and faster hydrolysis,[42] which is expressed in smaller k_+ and lower k_- for pH = 7.2 than for 6.1. This change in reactivity explains in turn, why we need more fuel for the same drop in radius for pH = 7.2. Moreover, we find excellent agreement between the saturation concentration p_{sat} when compared to the experimental numbers.[16]

Of special interest is the behavior of the duration of the transient times and how they are controlled by the physical and
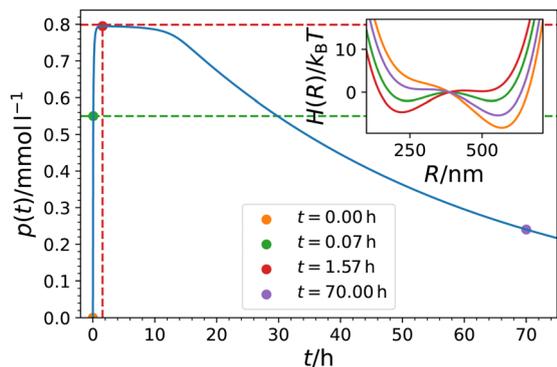
Fig. 4 Model prediction of the temporal evolution of the product concentration $p(t)$ in the system of Heckel et al.[16] Parameters were taken from Table 2 (pH = 6.1, $f_0 = 0.99$ mmol l^{-1}). The colored symbols depict different times for which the bimodal landscape $\mathcal{H}(Q)$ is plotted in the inset using the same color code. The values of p_{sat} and p^* are indicated by horizontal red and green dashed lines, respectively. The time of the maximum t_{max}, when $p(t_{max}) = p_{sat} = p_{max}$, is indicated by the red vertical line.

chemical parameters in the system. In the experimental paper[16] the transient times were defined as the timespans between $R^* = (R(t = 0) + R_{min})/2$, where R_{min} is the minimum radius for each individual curve. We denote this half collapse time by $\tau_{1/2}$ in the following. This definition we can in principle also apply to the data generated by our model.

However, we evaluate the transient times, τ_{trans}, in our model according to our well-defined symmetry definition eqn (15), which is similar but not exactly the same as $\tau_{1/2}$. The definition is applied to the fitting curves in Fig. 3 and plotted vs. f_0 in Fig. 5, in which we compare also to the experimental definition $\tau_{1/2}$. There is overall very good agreement. In particular, this plot suggests a linear connection between τ and f_0, as predicted from our analysis of the transient times in the saturated plateau regime, eqn (20). Using the fitted values in Table 2 we obtain slopes of 1.01×10^5 and 3.59×10^4 h l mmol^{-1} for pH = 6.1 and 7.2, respectively. They
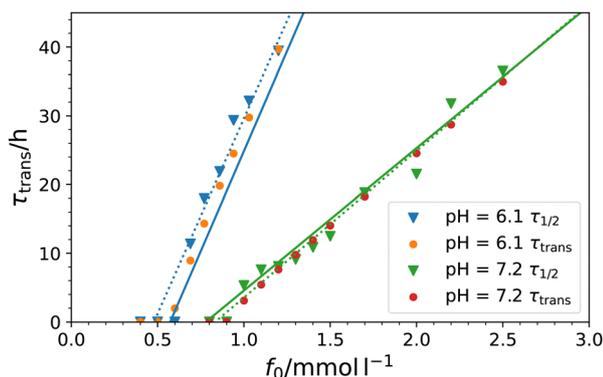

Fig. 5 Duration times of transient states, τ_{trans}, eqn (15), for both pH-values in dependency of the initial fuel concentration f_0 (solid circles) compared to the experimentally evaluated times $\tau_{1/2}$[16] (filled triangles, fitted linearly by the dotted lines). The solid lines show slopes calculated by the theoretical 'plateau regime' prediction, eqn (20), with y-intercept fixed consistently with $\tau(p^*) = 0$ (cf. eqn (24)) with p^* from Table 2.

are shown as straight lines in Fig. 5 where the y-intercept is chosen consistently from our fits where $\tau(p^*) = 0$, i.e., where activation of the transient state starts:

$$\tau(p) = \frac{1}{k_- p_{sat}}(p - p^*) \qquad (24)$$

Linear fits of the experimental $\tau_{1/2}$ provide 9.83×10^4 and 3.70×10^4 h l mmol^{-1} (dotted lines) underlining the agreement between experiment and theory. Hence, we understand the linear relation between $\tau_{1/2}$ and f_0 described by Heckel et al.[16] in a mathematical framework, which facilitates lifetime tuning of the transient state.

C. Thermodynamic analysis in the QS limit

In the QS limit, thermodynamic quantities such as energy, entropy, etc., are time-dependent but still well defined. For selected parameters (cf. Table 2, at pH = 6.1, $f_0 = 0.99$ mmol l^{-1}) we show $U(t)$, $S(t)$ and the free energy $F(t)$ in Fig. 6. We have already discussed $F(p)$ and found that it has a maximum at $p(t) = p^*$ where the Hamiltonian is symmetric and which is realized two times in the system: at very short times ($t \simeq 0$ on this linear scale; see Fig. S8 in ESI† for logarithmic time scales) where $F(t)$ jumps up and down in a δ-peak like fashion and again at about $t \simeq 30$ h. (Note that if we do not reach the transient state because $p_{max} < p^*$, then F would only have one maximum.) The behavior of $F(t)$ looks complex, since F drops to a local minimum between the two maxima, at which we have the transient plateau behavior, during which $p \simeq p_{sat} = p_{max}$. After the second maximum $F(t)$ relaxes back to the initial state. The apparently complexity essentially arises from the mapping of the asymmetric chemical kinetics $p(t)$ on the behavior of $F(p)$ according to the bistable Hamiltonian, eqn (1). As one can see in Fig. 6(a), U and S have similar functional forms than F. For an unimodal Hamiltonian less complex behavior can be expected.

The inset of Fig. 6(a) shows the derivative of the free energy, $P = dF/dt$, which we can interpret as the thermodynamic power. It has its largest absolute values immediately at the addition of the fuel at $t = 0$, meaning that the system is most active initially. This makes sense given the high k_+ to k_- ratio. It can also be understood from the analytical results, eqn (9) which is largest at the beginning where the radius is biggest and products massively produced, $P(t = 0) \simeq mf_0 k_+(Q_2 - Q_c)$. For later times during relaxation then broader and flatter peaks in the power develop at around $t \simeq 30$ h, when $F(t)$ peaks again and the system transitions back to the initial state. Hence, most work is performed chemically and elastically at the transitions to and from the transient state in a bistable system. The same qualitative behavior is exhibited by the entropy production (see Fig. S7 in ESI†).

Part (b) of Fig. 6 displays the course of the total energy $U(t)$ and its mechanical and chemical contributions, U_0 and U_{chem}, respectively. The most intuitive is the mechanical energy U_0. By addition of the fuel we force the hydrogel very quickly to the collapsed state whereby energy is stored (increased) elastically. Its time of maximum coincides with that of maximum products, $p = p_{sat}$, and then we observe relaxation, where the stored
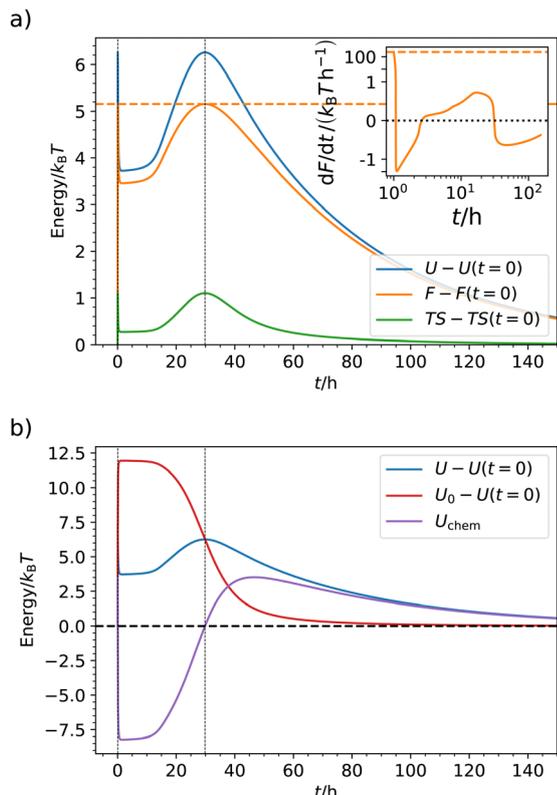
a)

b)

Fig. 6 (a) Temporal evolution of the energy $U(t)$, free energy $F(t)$ and entropic contribution $TS(t)$ subtracted by their initial values at time $t = 0$ for $f_0 = 0.99$ mmol l^{-1} and parameters taken from Table 2 at pH = 6.1. The maximum of F given by eqn (19) is marked by the horizontal dashed (orange) while the vertical dotted lines mark the two times where $p = p^*$. The inset shows the power (work per time, $P = dF/dt$) as a function of t (with time axis shifted by 1 h to allow for a logarithmic scale. Because of negative values of P, the scale on the y-axis is linear between -0.01 and $0.01 k_B T$ h^{-1} and logarithmic elsewhere. For the negative part, we show $-\log(-P)$). The horizontal dashed line shows the analytical limit of eq. (9) at $t = 0$. (b) The total energy U split in mechanical (U_0) and chemical contributions (U_{chem}) according to eqn (12) and (13). Plots with logarithmic time-axis can be found in in Fig. S8 ESI†

energy is released again. For the total U, the shape is different. Here, we observe the maxima as in $F(t)$ where $p = p^*$, otherwise the energy is always lower. To understand this, let us consider the chemical (or external) part U_{chem}, being the difference of U and U_0: it increases δ-peak like in the very beginning ($t \simeq 0$ on this scale) when chemical energy is quickly pumped into the system and converted to mechanical one. When the mechanical energy starts relaxing, U_{chem} rapidly decreases and turns negative. Subsequently, the process is reversed but not chemically fueled, driven by the stored elastic energy. Note that U_{chem} has zeros at short times $p(t) \simeq 0$ (on this scale) and at $p(t) = p^*$. This is accompanied with maxima in the entropy, *cf.* Fig. 6(a), indicating heat exchange with the bath along the evolution of the internal energy.

D. Effects of slow system relaxation

We finally discuss the effects of slow relaxation, such as possible delays in the system's response,[22] in the context of

the just discussed case of chemically fueled hydrogel collapse. For this, we fix the parameters according to Table 2, for pH = 6.1 and $f_0 = 0.99$ mmol l^{-1}. We now tune the timescale separation parameter α in eqn (22) from 0.1 to 10 and solve numerically the Smoluchowski eqn (21) for the distribution $\rho(Q,t)$ to calculate averages, such as $R(t)$. The results are shown in Fig. 7(a). For $\alpha = 0.1$ we are still very close to the QS limit because the diffusive system relaxation is still 10-fold faster than the fast rate k_+. However, moving to $\alpha = 0.5$ or 1, we observe clear retardation effects, involving less collapse and a delay of the minimum in time. For $\alpha = 5$ and larger, the system becomes quite inert and the response effects less and less pronounced. The chemical power transforms mostly into dissipative losses and cannot be used to perform work. Clearly, a change of internal timescales can change the nonequilibrium time evolution and thermodynamics massively.

In the just described system we have still a relatively small barrier of $\Delta \mathcal{H} = 2 k_B T$. If we raise the barrier, the system relaxation time should be more adequately described by the Kramers crossing time, eqn (23), leading to the time scale ratio
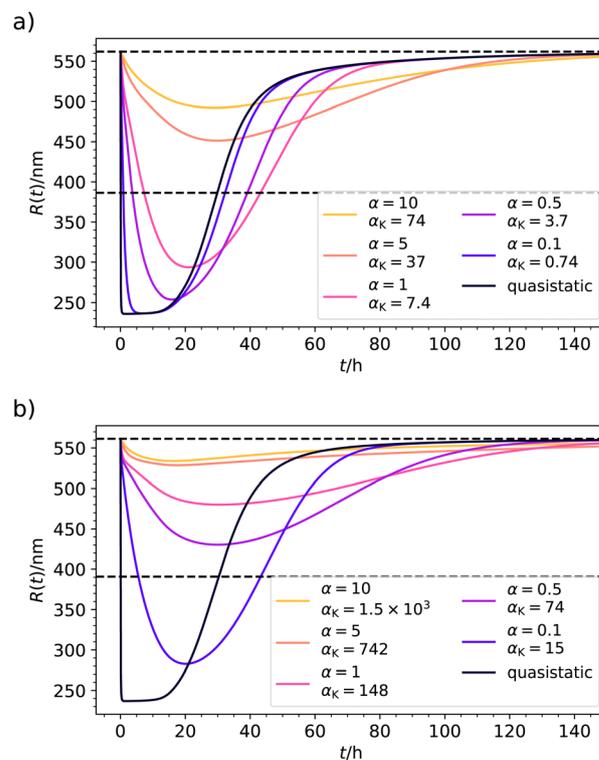
a)

b)

Fig. 7 (a) Exemplary results for the time evolution of hydrogel radius $R(t)$ in the case of slow system relaxation calculated from the Smoluchowski approach. Values for the energy landscape were taken from Table 2 (for pH = 6.1, $f_0 = 0.99$ mmol l^{-1}). The timescale ratio $\alpha = \tau_D k_+$ defines the ratio of a typical system diffusion time and the chemical timescale k_+^{-1}. Additionally, we provide the Kramers reference α_K defined by eqn (23). For very fast relaxation $\alpha \ll 1$ we reach the QS limit. By the horizontal dashed lines we show the radius before fueling $R(t = 0)$ and the threshold radius $R(p^*)$. (b) Same as (a) but now the parameters are chosen such that the transition barrier is increased from $2 k_B T$ to $5 k_B T$. Here, the system relaxation is too sluggish for the considered α from which we can deduce that α_K provides the more precise time scale estimate.

$\alpha_K = \tau_{\text{Kramer}} k_+$. This is exemplified in Fig. 7(b) where we use the alternative fit with a barrier height of $\Delta\mathcal{H} = 5 k_B T$. The Kramers time is now about 150 times larger than τ_D resulting, for example, in $\alpha_K = 15$ for $\alpha = 0.1$ for a response which is already clearly non-QS (brown curve in Fig. 7(b)). Hence, the Kramers time is naturally more appropriate to characterize delayed systems involving internal barriers. (Results with a slightly different definition of the Kramers time based on energy landscape curvatures time shown in Fig. S9 in the ESI† do not change our conclusion.)

IV. Concluding remarks

In this contribution, we have put forward a Landau type of mean-field model to describe the quasi-static and nonequilibrium chemical fueling of transient states (CFTS) in a bistable system. Already the analysis of the quasi-static (QS) limit led to useful scaling laws and relations between chemical and mechanical parameters, which could serve for the future design of experiments. We demonstrated their usefulness explicitly for the case study of the chemically fueled volume (collapse) transition of responsive hydrogel colloids. Moreover, we provided a thermodynamic (energy, work, and power) analysis in the QS limit and also showed how internal (diffusive) relaxation times scales can substantially alter the time evolution if they compete with the chemical timescales of fueling.

Several extensions of this model for CFTS shall be interesting in future studies. In our manuscript we focused on the induction and relaxation of the collapsed state, following a simple two-step reaction. If a continuous supply of fuel could be realized, e.g., as in a flow reactor, one could expect that the hydrogel would initially monotonically reach and then remain in the collapsed state. Generally, the question becomes important, how can we define chemical reaction (networks) and/or experimental protocols to program a pre-defined time-dependent macroscopic response into the system. Also, by including more complex order parameters, higher dimensions of the reaction coordinate, or structural gradients in the Hamiltonian, the extension and application of our model to self-assembling[12] and phase separating systems[14,15] could be attempted. From the chemical side, as indicated above, higher order reaction networks[8,20,43] than only two-step reactions could be envisioned. Finally, further increasing complexity could be obtained by imposing a negative feedback cycle within the system, e.g., by coupling the mechanical response back to the chemical reaction.[44–46] Here, much more intricate transient dynamics and responses, including regimes of mono- and bistability, excitability, damped oscillations, as well as sustained oscillatory states can be expected during the time evolution.[8,47]

Conflicts of interest

There are no conflicts to declare.

Acknowledgements

References

1 A. Desai and T. J. Mitchison, *Annu. Rev. Cell Dev. Biol.*, 1997, **13**, 83–117.

2 G. M. Whitesides and B. Grzybowski, *Science*, 2002, **295**, 2418–2421.

3 V. V. Yashin, K. J. Van Vliet and A. C. Balazs, *Phys. Rev. E*, 2009, **79**, 046214.

4 A. P. Dhanarajan, G. P. Misra and R. A. Siegel, *J. Phys. Chem. A*, 2002, **106**, 8835–8838.

5 R. Merindol and A. Walther, *Chem. Soc. Rev.*, 2017, **46**, 5588–5619.

6 A. Walther, *Adv. Mater.*, 2020, **32**, 1905111.

7 Q. Wang, Z. Qi, M. Chen and D.-H. Qu, *Aggregate*, 2021, **2**, e110.

8 A. V. Straube, S. Winkelmann, C. Schütte and F. Höfling, *J. Phys. Chem. Lett.*, 2021, **12**, 9888–9893.

9 D. M. Busiello, S. Liang, F. Piazza and P. De Los Rios, *Communi. Chem.*, 2021, **4**, 16.

10 A. Sharko, D. Livitz, S. De Piccoli, K. J. M. Bishop and T. M. Hermans, *Chem. Rev.*, 2022, **122**, 11759–11777.

11 J. Boekhoven, W. Hendriksen, G. Koper, R. Eelkema and J. van Esch, *Science*, 2015, **349**, 1075–1079.

12 T. Heuser, E. Weyandt and A. Walther, *Angew. Chem., Int. Ed.*, 2015, **54**, 13258–13262.

13 S. Panja, C. Patterson and D. J. Adams, *Macromol. Rapid Commun.*, 2019, **40**, 1900251.

14 J. Deng and A. Walther, *Chem*, 2020, **6**, 3329–3343.

15 J. Heckel, F. Batti, R. T. Mathers and A. Walther, *Soft Matter*, 2021, **17**, 5401–5409.

16 J. Heckel, S. Loescher, R. T. Mathers and A. Walther, *Angew. Chem., Int. Ed.*, 2021, **60**, 7117–7125.

17 M. Nakamoto, S. Kitano and M. Matsusaki, *Angew. Chem., Int. Ed.*, 2022, **61**, e202205125.

18 L. Heinen and A. Walther, *Sci. Adv.*, 2019, **5**, eaaw0590.

19 H. Zhang, H. Zeng, A. Priimagi and O. Ikkala, *Nat. Commun.*, 2019, **10**, 3267.

20 B. Klemm, R. W. Lewis, I. Piergentili and R. Eelkema, *Nat. Commun.*, 2022, **13**, 6242.

21 L. Ionov, *Mater. Today*, 2014, **17**, 494–503.

22 G. Fusi, D. Del Giudice, O. Skarsetz, S. Di Stefano and A. Walther, *Adv. Mater.*, 2023, **35**, 2209870.

23 X. He, M. Aizenberg, O. Kuksenok, L. D. Zarzar, A. Shastri, A. C. Balazs and J. Aizenberg, *Nature*, 2012, **487**, 214–218.

24 S. G. J. Postma, I. N. Vialshin, C. Y. Gerritsen, M. Bao and W. T. S. Huck, *Angew. Chem., Int. Ed.*, 2017, **56**, 1794–1798.

25 P. Hohenberg and A. Krekhov, *Phys. Rep.*, 2015, **572**, 1–42.

26 C. N. Pace, *CRC Crit. Rev. Biochem.*, 1975, **3**, 1–43.

27 J. A. Schellman, *Biopolymers*, 1978, **17**, 1305–1322.

28 J. Heyda and J. Dzubiella, *J. Phys. Chem. B*, 2014, **118**, 10979–10988.

29 J. Heyda, S. Soll, J. Yuan and J. Dzubiella, *Macromolecules*, 2014, **47**, 2096–2102.

30 R. Elancheliyan, G. Del Monte, E. Chauveau, S. Sennato, E. Zaccarelli and D. Truzzolillo, *Macromolecules*, 2022, **55**, 7526–7539.

31 M. A. Fernandez-Rodriguez, S. Orozco-Barrera, W. Sun, F. Gámez, C. Caro, M. L. García-Martín and R. A. Rica, *Small*, 2023, 2301653.

32 I. Langmuir, *J. Am. Chem. Soc.*, 1918, **40**, 1361–1403.

33 H. Bateman, *Proc. Cambridge Philos. Soc.*, 1910, **15**, 423–427.

34 M. Doi and S. F. Edwards, *The Theory of Polymer Dynamics*, Oxford University Press, 1988.

35 H. Risken, *The Fokker-Planck equation*, Springer, 1996.

36 V. Holubec, K. Kroy and S. Steffenoni, *Phys. Rev. E*, 2019, **99**, 032117.

37 H. S. Fogler, *Elements of Chemical Reaction Engineering*, Prentice Hall, 4th edn, 2005.

38 H. Kramers, *Physica*, 1940, **7**, 284–304.

39 P. Hänggi, P. Talkner and M. Borkovec, *Rev. Mod. Phys.*, 1990, **62**, 251–341.

40 L. S. Kariyawasam, J. C. Kron, R. Jiang, A. J. Sommer and C. S. Hartley, *J. Organic Chem.*, 2020, **85**, 682–690.

41 A. Williams and I. T. Ibrahim, *J. Am. Chem. Soc.*, 1981, **103**, 7090–7095.

42 C. W. Woodruff, G. E. Peck and G. S. Banker, *J. Pharm. Sci.*, 1972, **61**, 1916–1921.

43 J. Deng and A. Walther, *Nat. Commun.*, 2021, **12**, 5132.

44 B. Li and R. A. Siegel, *Chaos*, 2000, **10**, 682.

45 D. J. Bell, D. Felder, W. G. von Westarp and M. Wessling, *Soft Matter*, 2021, **17**, 592–599.

46 M. Jain and B. J. Ravoo, *Angew. Chem., Int. Ed.*, 2021, **60**, 21062–21068.

47 S. Milster, N. Göth, A. Darwish and J. Dzubiella, *Phys. Rev. E*, 2023, **108**, https://arxiv.org/abs/2306.05181.